Indian Journal of Pure & Applied Physics
Vol. 64, January 2026, pp. 76-97
DOI: 10.56042/ijpap.v64i1.24305

# Adaptive Hybrid PO and Drone Squadron Optimization MPPT Tecnique for Solar PV Systems Under Diverse Conditions

Rahul Kumar Rai* & Umesh Kumar Sinha

Department of Electrical Engineering, National Institute of Technology Jamshedpur, 831 014, India

*Received: 1st October 2025; accepted: 3rd November 2025*

Recent studies on solar photovoltaic (PV) system aim to make the system more efficient and generally, the performance of the PV arrays. A key aim is to reduce energy losses that arise due to variable weather patterns and irregular load demands. Traditional approaches include Perturb and Observe (PO) which are easy and work well when there is a stable setting, often fail under partial shading conditions (PSC). This paper proposes a hybrid MPPT approach that integrates Perturb and Observe (PO) with Drone Squadron Optimization (DSO) to improve the performance of solar PV systems under varying environmental conditions. The proposed hybrid PO–DSO method combines the fast response of PO with the global search capability of DSO, allowing the system to avoid local optima and accurately track the Global Maximum Power Point (GMPP). A comprehensive simulation study was conducted in different scenarios as constant irradiance, temperature variation, and partial shading. At constant irradiance case, the proposed algorithm achieved a PV power output of 249.5 W and delivered 243.68 W to the load. Under temperature variation, it maintained a high output of 249.3 W, demonstrating thermal stability. During PSC, it successfully tracked the GMPP with PV output of 128.25 W & 128.3 W and a load power of 124.31 W & 124.2 W. Comparative analysis with particle swarm optimization (PSO), cuckoo search algorithm (CS) and flower pollination algorithm (FPA) showed that the proposed method achieved the highest tracking efficiency of up to 99.8 %, with faster convergence and fewer oscillations. These results highlight the hybrid method's robustness, making it a promising MPPT solution for real-world PV systems operating in unpredictable and dynamic weather conditions. Lastly, the viability and validation of the use of the approach and its applicability in practice were tested through real-time simulation on the OPAL-RT platform.

**Keywords:** Grid-linked PV scheme, Zeta converter, Incremental conductance MPPT, DC link voltage, Voltage regulation, Renewable energy, Solar photovoltaic

## 1 Introduction

Renewable energy systems are also being known as reliable and effective solutions in improving the electricity access in the whole world. As more environmental challenges have been grown and the world has slowly depleted its fossil fuel reserves, these systems have become the new technological remedy to the traditional methods of power production and have been playing a significant role in the progress of the sustainable development[1-4]. The solar energy is one of the renewable energies that are the most abundant and accessible. It will be easily harnessed with the aid of photovoltaic (PV) panels or solar thermal systems that are aimed at transforming sunlight into useful energy[5-6]. Photovoltaic systems, when integrated into electrical grids, stands out as one of the most dependable and efficient renewable energy sources available today. It offers a clean, abundant, and cost-effective means of power generation, contributing significantly to sustainable economic growth and job creation[7-8]. PV technology have advanced significantly as a result of the growing need for non-conventional resources worldwide. To extract maximum power under all conditions, however, MPPT procedures are required because to the nonlinear nature of PV systems and their reliance on environmental factors like temperature and sun irradiation. Traditional MPPT procedures, like P&O, are straightforward and efficient in steady-state situations, but they perform poorly in dynamic ones, particularly when there is PSC or quickly changing weather, where several local maxima can trick simple algorithms. PV modules design and modeling have been extensively studied, especially in relation to the impact of environmental factors on performance. Several research works exist in the field of solar energy, the primary areas of investigations & findings generally include analysis of maximum power point tracking (MPPT) methods, reconfiguration strategies for PV arrays, modeling & analysis of solar cell

*Corresponding author: E-mail: rahul.rai751@gmail.com

characteristics, methods for enhancing system efficiency and integration with the power grid[9-14]. The equivalent circuit model, which has both series and parallel resistances to increase accuracy, is a frequently used technique[15]. This model aids in simulating how PV modules will behave electrically when exposed to varying temperatures and irradiance levels. Through simulation of the PV system using tools such as MATLAB/Simulink, researchers have evaluated the impact of fluctuating weather data and identified the ideal resistance settings to get the highest output. A substantial amount of research has been conducted on MPPT procedures concurrently with modeling efforts, particularly in situations when the P-V curve displays several peaks due to PSC. Four major categories have been identified by researchers for MPPT methodologies: control-oriented converter topologies, sophisticated modeling techniques, hybrid strategies, and optimization-based methods. The advantages and disadvantages of each algorithm can be more systematically assessed thanks to this classification. It also emphasizes importance to choose methods carefully when developing PV systems that will be exposed to environmental uncertainty and shade in the actual world[16]. Smart optimization methods like as CS and PSO have shown promise in extracting the global MPP under PSC. The convergence and tracking accuracy of these techniques has significantly improved as compared to more traditional methods like incremental conductance. Particularly, CS has proven to be more accurate and track more quickly than PSO in a variety of simulated shade patterns, which makes it a good option for intricate PV scenarios[17]. In addition to categorizing MPPT techniques, a number of evaluations have highlighted the significance of assessing their usefulness in real-world scenarios using hardware simulations and algorithm-specific design. The division of control techniques into measurement-based, computational, smart, and hybrid categories provides a thorough framework for choosing the best algorithm based on system design and financial limitations. Additionally, the incorporation of hybrid controllers and fuzzy logic into conventional methods has enhanced robustness in dynamic operating situations[18]. Conventional MPPT methods, like PO and voltage/current-based approaches, frequently fail to converge to the global maximum under rapidly changing irradiance and temperature profiles, especially when there are several local peaks. To get around this, sophisticated optimization techniques like PSO have been put forth, and they have demonstrated notable performance improvements. These methods have been demonstrated to perform better than traditional methods in both steady and transient situations, and they are especially useful for negotiating the non-linearities brought about by partial shading[19]. To further strengthen PSO-based approaches, changes have been made to raise convergence speed and eliminate tracking fluctuations. Some recent advancements include the assessment of the curving area of the P-V curve, which helps lead the algorithm more efficiently toward the global MPP. These changes have been validated through experimental and simulation experiments, revealing that the upgraded PSO variants maintain stability and achieve faster response times across diverse partial shading circumstances. The versatility of such techniques makes them well-suited for implementation in grid-linked PV schemes where consistency and reliability are essential[20]. Recent research has progressively stressed the necessity for more accurate and responsive MPPT algorithms in PV systems, particularly in dynamic and partially shadowed conditions. To address the constraints of conventional methods that often fail to pinpoint the GMPP, researchers have proposed hybrid and intelligent approaches. One such strategy is the merging of CS and PSO to develop a hybrid CSPSO technique. This approach combines the global exploration capabilities of CS with the quick convergence characteristic of PSO to accurately trace the GMPP. Simulation studies across diverse irradiance profiles and PV setups reveal that the CSPSO surpasses individual metaheuristic approaches in terms of accuracy, convergence speed, and total tracing efficiency[21]. Similarly, the deployment of standalone CS in MPPT has produced good outcomes. By lowering tracking time and boosting accuracy, CS has showed greater performance when benchmarked against traditional techniques like PO. Its implementation utilizing a boost regulator arrangement in MATLAB/Simulink confirms its resilience and appropriateness for practical PV schemes[22]. Meanwhile, the FPA, another metaheuristic technique, has also attracted attention for its capacity to sustain consistent tracking throughout difficult PSC. Utilizing Levy flight to boost search variety, FPA has been demonstrated to give excellent tracking accuracy and faster convergence across variable temperature and irradiance conditions, with strong statistical performance metrics in real-world simulations[23]. In addition to designing unique algorithms, academics have also concentrated on enhancing conventional ones. An enhanced version of the PO approach has been presented, combining dynamic perturbation step sizes and boundary conditions. This approach lowers steady-state oscillations and prevents divergence from the MPP. It requires little adjustments to existing systems, delivering a low-cost upgrade appropriate for application in buck-boost converters. Evaluations employing varied irradiance profiles demonstrate that the improved PO consistently delivers greater MPPT efficiency than conventional versions[24]. A more recent invention in global optimization is the DSO approach. Unlike nature-inspired algorithms, DSO is artifact-inspired and employs a command-control architecture integrating semi-autonomous drones and a dynamic firmware update mechanism. This self-adaptive method has shown competitive performance when tested on benchmark functions and gives a versatile framework for optimization in PV applications. The perturbation approach utilized in DSO is continuously modified during runtime, allowing the approach to adapt effectively to the optimization terrain[25]. Another study has used this technique, which builds on DSO, in the context of hybrid PV-Battery scheme. The study highlighted the necessity of strong energy control in schemes with variable solar input and limited battery specifications. The suggested approach effectively tracks the GMPP under different partial shade patterns and guarantees dependable grid interaction by integrating DSO. In order to improve system resilience and maximize energy use in grid-linked rooftop PV systems, the study also investigates energy distribution techniques and battery behavior models[26]. The majority of current methods still struggle to achieve quick, stable convergence under combined temperature and irradiance variations, even with improvements in metaheuristic and hybrid MPPT algorithms. Few studies balance the two in dynamic real-time contexts; most concentrate on either optimization accuracy or response time.

The major contribution of the proposed research are summarized as: -

i A novel hybrid PO-DSO MPPT algorithm has been developed and implemented for solar PV systems to enhance tracking speed and efficiency.

ii The performance of the proposed algorithm was examined under various environmental conditions and compared with various algorithms like PSO, CS, and FPA.

iii Different test scenarios including fixed irradiance, temperature variation, and Partial shading conditions, are taken to assess the performance of the proposed hybrid MPPT. The proposed method achieves a less tracking time, high efficiency with very low voltage and current ripple in each case.

iv To evaluate robustness, the system was tested under dynamic weather conditions with random insolation and temperature with probabilistic load, examining parameters such as tracking speed, efficiency, voltage and current ripple, power output, energy losses, and error indices. The proposed method demonstrated less average response time to achieve MPP, maintaining tracking efficiency of nearly 99 % and overall efficiency of around 96-98% across all scenarios with reduced power losses.

v Additionally, the proposed hybrid approach was experimentally validated in a real-time laboratory setup using the OPAL-RT (OP2410) simulator, confirming its effectiveness and reliability.

## 2 System Description

A PV system with a Hybrid PO–DSO MPPT controller integrated to harvest maximum power is presented in Fig. 1. The first component of the arrangement is a PV array, which generates output voltage and current by converting solar radiation into electrical power. The hybrid MPPT controller block receives these parameters as input.

The MPPT controller employs a hybrid algorithm that adds the intelligent search capabilities of the Drone Squadron Optimization methodology with the conventional Perturb and Observe method. This

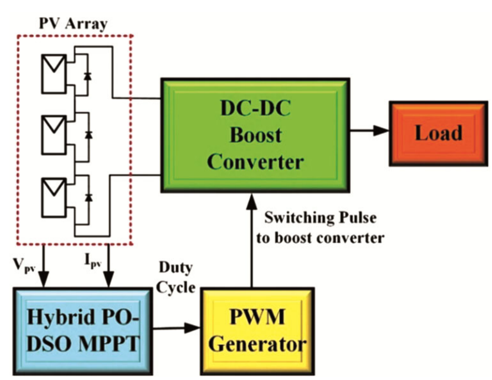


Fig. 1 — Overall system Architecture

hybrid approach improves MPPT speed and accuracy, particularly in situations with fluctuating irradiance, such as partial shading. The Hybrid PO–DSO MPPT controller uses the power point to identify the ideal duty cycle. It then transmits this information to the PWM generator, which transforms it into matching switching pulses. A boost regulator which modifies the PV output voltage and makes sure the system runs at or close to the maximum power point (MPP), is controlled by these pulses. The load is subsequently supplied with the converter's regulated DC power. Effective power transfer from the PV to the linked load and dynamic tracking of the MPP are guaranteed by this closed-loop control system.

### 2.1 Modeling of Solar PV

PV cells use the photovoltaic effect to convert radiation into electrical energy. Current is produced when sunlight strikes a photovoltaic module because the photon energy is higher than the semiconductor's bandgap, releasing charge carriers (electrons and holes).

The PV cell specification is given in Table 1 with their symbol and value. The equivalent circuit of a PV cell (Fig. 2) comprises a light-driven current source $I_{pv}$ that models the photo-generated electron flow, a diode D that captures the nonlinear p–n junction behavior, a shunt resistance $R_p$ that represents leakage currents across the junction, and a series resistance $R_{se}$ that accounts for ohmic losses in the semiconductor material and its contacts. The output current Io delivered by the PV cell is expressed as,

$$I_o = I_{pv} - I_D - I_p \quad \ldots (1)$$

The diode current follows the Shockley diode equation,

Table 1 — PV cell specifications

| Parameters | Value |
|---|---|
| Series Resistance value ($R_s$) | 0.09862 Ω |
| Shunt Resistance value ($R_{sh}$) | 82.1161 Ω |
| Value of Short circuit current ($I_{sc}$) | 8.62 A |
| Open circuit voltage value ($V_{oc}$) | 37.92 V |
| Rated Current ($I_M$) | 8.07 A |
| Rated Voltage ($V_m$) | 30.96 V |
| Rated power ($P_m$) | 249.8472 W |
| Cells per module | 60 |
| No. of series module | 1 |
| No. of parallel module | 1 |
| Temp. Coeff. Of Voc (%/deg.c) | -0.33969 |
| Temp. Coeff. Of Voc (%/deg.c) | 0.063701 |

$$I_D = I_o\left(e^{\frac{q(V_O+I_O R_{se})}{nkT}} - 1\right) \quad \ldots (2)$$

In this model, $I_o$ denotes the reverse saturation current of the diode. The parameter q represents the fundamental charge of an electron. The output voltage across the PV terminals is indicated by $V_o$ , while $R_{se}$ models the internal series resistance that causes voltage drops within the cell. The diode ideality factor, n, k stands for Boltzmann's constant, T represents the absolute temperature of the cell in Kelvin, which significantly affects the overall current-voltage characteristics. Figure 3 presents the IV & PV characteristics of PV.

The photocurrent $I_{pv}$ is dependent on temperature and irradiance and is modeled as,

$$I_{pv} = \frac{G}{G_o}[I_{sc} + \alpha(T - T_o)] \quad \ldots (3)$$

Here, $I_{sc}$ denotes the short-circuit current. The variables G and $G_0$ represent the actual and reference levels of solar irradiance, respectively, indicating the intensity of sunlight incident on the PV module. Similarly, T and $T_0$ refer to the actual operating temperature and the standard reference temperature. The parameter α is the temperature coefficient of short-circuit current, substituting Eqs (2) and (3) into Eq. (1), the full nonlinear model becomes,

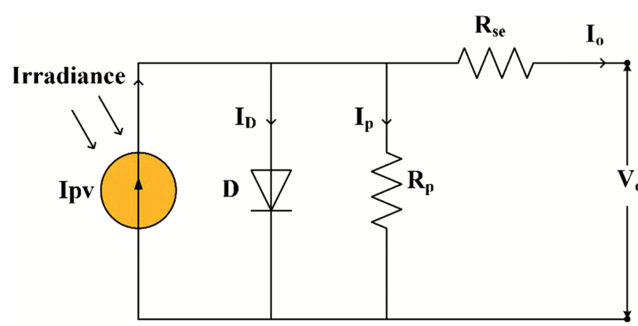


Fig. 2 — PV Equivalent circuit

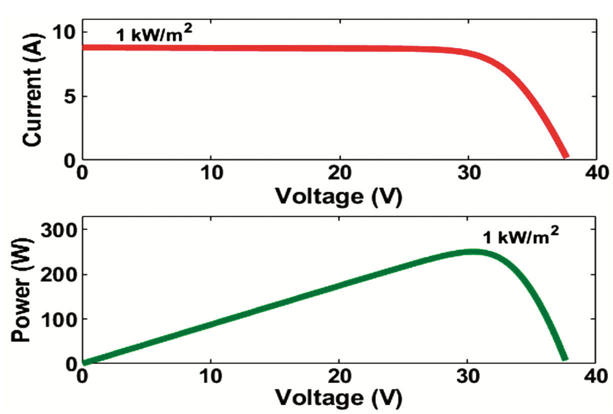


Fig. 3 — I-V & P-V characteristics of PV array

$$I_o = \frac{G}{G_o}[I_{sc} + \alpha(T - T_o)] - I_o\left(e^{\frac{q(V_o+I_oR_{se})}{nkT}} - 1\right) - \frac{V_o+I_oR_{se}}{R_p} \quad \ldots (4)$$

### 2.2 Effect of PSC

In a PV array, each PV module experiencing the equal amount of sunlight under the condition of constant insolation, and the power produced by array will remain constant. However, during PSC resulting from clouds, bird droppings, nearby objects, trees, or dust may block some parts of the PV module, resulting in uneven distribution of insolation on the PV array. Hence, the PV cells' power outputs differ, causing the P-V curve to have several local maxima. While the others are referred to as LMPP, the highest peak is known as the GMPP. Bypass diodes are inserted across each PV modules to mitigate the mismatch impact that arise under PSC. When certain modules are shaded, these diodes provide an alternate pathway for the excess current generated by unshaded modules, thereby preventing the development of hotspots, maintaining uninterrupted current flow, and reducing efficiency losses across the system. The presence of many peaks in the P-V curve under PSC demands a robust MPPT algorithm capable of detecting and tracking the GMPP effectively. As, PV array shows nonlinear behavior operating under partial shading condition (PSC), produces multiple number of peaks in the power-voltage(P-V) characteristics. Among the generated peaks, the lower peaks are identified as local maximum power points (LMPP), whereas the absolute highest point is identified as the global maximum power point (GMPP). Accurate identification of the GMPP is critical, as conventional tracking techniques often get trapped at an LMPP, leading to considerable power loss. To mitigate mismatch effects introduced by shading, bypass diodes are strategically connected across each PV module. These diodes offer an alternate pathway for the excess current generated by unshaded modules, which serves three essential purposes: preventing the development of localized hotspots, maintaining a continuous current path throughout the array, and minimizing efficiency degradation. Despite the use of bypass diodes, the challenge of multiple peaks in the P–V profile remains, particularly under rapidly changing irradiance. This necessitates the development of advanced maximum power point tracking (MPPT) strategies that not only distinguish the GMPP from nearby LMPPs but also demonstrate robustness, fast convergence, and adaptability to dynamic environmental conditions. The condition for maximum power extraction can be mathematically defined as:

$$\frac{dp}{dV_{pv}} = \begin{cases} = 0, at\ MPP \\ > 0, to\ the\ left\ of\ MPP \\ > 0, to\ the\ right\ of\ MPP \end{cases} \quad \ldots (5)$$

Therefore, the selection of an effective MPPT controller significantly impacts the overall system efficiency. In this study, a new hybrid PO-DSO-based MPPT method is presented to track the GMPP under PSC with high tracking accuracy.

## 3 Methods and Materials

### 3.1 Proposed MPPT Control Scheme

A hybrid MPPT control design that combines the DSO and P&O methods to ascertain the ideal duty cycle for a boost regulator is shown in Fig. 4. Both MPPT blocks receive the Vpv and Ipv at the same time. Based on their own strategies, each algorithm separately determines a duty cycle. PO tracks locally around the current operating point, whereas DSO offers worldwide search capabilities. A refined duty cycle is produced by combining the outputs from the DSO MPPT and PO MPPT blocks using an averaging or weighted mechanism. The PWM generator then receives this combined value and generates the matching switching pulses for the boost regulator. The system delivers better tracking accuracy, faster convergence, and increased performance under dynamic conditions like partial shade or variable irradiance by utilizing the advantages of both methods.

#### *3.1.1 PO MPPT*

This method is simple and effective under uniform irradiance, but it can get trapped in local maxima under PSC. The Perturb and Observe (PO) algorithm is a classical hill-climbing method widely employed for maximum power point tracking (MPPT) in photovoltaic systems. The approach functions by perturbing the operating voltage and monitoring the

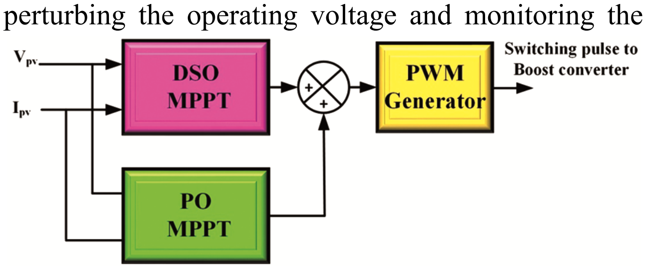


Fig. 4 — Representation of hybrid PO-DSO MPPT

resulting variation in power output; if the power increases, the algorithm continues in the same direction, whereas a decrease prompts a reversal of the perturbation to maintain convergence toward the maximum power point. The key operational components of the algorithm include real-time measurement of PV voltage and current, which are used to calculate instantaneous power, and a decision logic that compares current and previous power and voltage values ($P_{old}$, $V_{old}$) to determine whether the duty cycle should be incremented or decremented. Based on the slope of the PV power-voltage curve, small adjustments are applied to the duty cycle to ensure gradual convergence to the MPP, while boundary checks constrain the duty cycle within safe operational limits, typically between 0.08 and 0.95, to avoid instability or damage to the converter. While the simplicity and computational efficiency of the P&O method make it highly effective under uniform irradiance conditions, its performance can degrade significantly under partial shading, where multiple local maxima exist. In such scenarios, the algorithm may become trapped at a local optimum rather than reaching the true global MPP. Despite this limitation, PO remains a foundational MPPT technique, providing a straightforward and robust approach for systems where irradiance conditions are relatively stable and predictable.

#### *3.1.2 Drone Squadron Optimization (DSO)*

DSO is a metaheuristic procedure that draws its conceptual framework from the autonomous coordination and communication capabilities of modern drone swarms. These drones, akin to flying vehicles like helicopters or UAVs, can communicate over long distances, utilize solar energy, and are capable of both hardware and firmware self-upgrades. In DSO, the command center is the core controller responsible for generating firmware updates, coordinating search actions, and integrating knowledge gathered by drones during exploration. This modular structure is illustrated in Fig. 4, highlighting the interaction between drone teams and the command center.

i Command Center:

The Command Center is the "brain" of the DSO algorithm. Within the Drone Squadron Optimization (DSO) framework, the Command Center serves as the principal decision-making unit that directs the overall search process. Its role extends beyond simple coordination, as it systematically gathers performance feedback from each drone team and interprets this information through objective function evaluations. Based on these assessments, the Command Center updates and redistributes firmware to the drone teams, thereby refining their search trajectories in subsequent iterations. This continuous feedback adaptation cycle enables the algorithm to balance exploration and exploitation more effectively, improving convergence toward the global optimum. The process is guided by hyper-heuristic principles, in which a collection of low-level heuristics, such as perturbation based strategies, are arranged into a higher level decision making framework. Such integration ensures that firmware adjustments are not arbitrary but strategically aligned with the optimization goals, enhancing both robustness and adaptability in complex or dynamic problem environments. Command center & drone team in for DSO model is shown in Fig. 5.

ii Firmware and Perturbation Mechanism:

In the Drone Squadron Optimization (DSO) framework, the firmware installed within each drone plays a central role in defining its search dynamics. Beyond serving as a set of operational instructions, the firmware incorporates perturbation mechanisms that determine how new candidate solutions, known as trial coordinates (TCOD), are generated during the optimization process. This functionality is critical, as it governs the balance between exploration of the global search space and exploitation of regions that are likely to contain optimal solutions.

The basic perturbation model is expressed as:

$$M = Departure + Offset() \quad \ldots (6)$$

$$TCOD = Compute(M) \quad \ldots (7)$$

where, M denotes the perturbed movement vector, which is derived from a reference position termed the Departure coordinate. The function Offset () introduces controlled perturbations that are produced

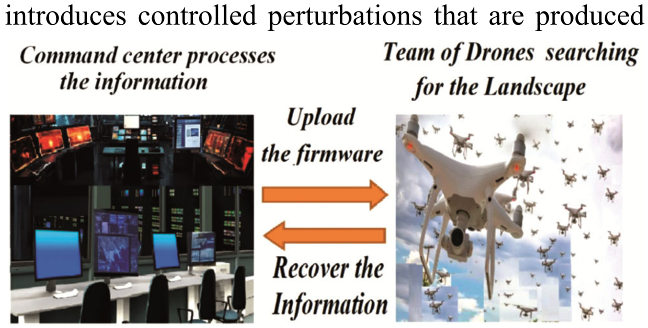


Fig. 5 — Command center & drone team in DSO model

through stochastic processes, ensuring the diversity in the search trajectories. The function Compute (M) then transforms the perturbed vector into a candidate trial coordinate, which is subsequently evaluated within the optimization cycle. By embedding such stochastic perturbation models within drone firmware, the algorithm achieves an adaptive balance between exploration of the global search space and exploitation of promising regions, ultimately enhancing convergence efficiency and robustness of the overall optimization procedure.

iii Drone Movement Strategy:

In the framework of Drone Squadron Optimization (DSO), each drone explores the search space independently to identify optimal solutions, often conceptualized as targets or prey. Upon reaching a candidate location, the drone evaluates the objective function to determine the quality of that point. The results are then transmitted to the Command Center, which collects information from all drones to guide subsequent search decisions. Drones operate within a predefined operational area, and any trial movement coordinates (TMC) that fall outside the permitted boundaries are corrected using repair mechanisms. These correction functions adjust coordinates back into the valid search region, ensuring that all candidate solutions remain feasible. For example, if a drone's proposed coordinate exceeds the upper limit of a dimension, the value is reset to the boundary, preserving adherence to constraints while allowing exploration to continue. This movement strategy enables several important aspects of the optimization process. It supports controlled stochastic exploration, allowing drones to perform random walks that maintain diversity in the search population. It also allows recombination of coordinates from other drone teams, incorporating shared information to generate improved trial solutions. Finally, by keeping the drone population diverse and avoiding repeated convergence on the same region, this strategy reduces the risk of premature convergence. Collectively, autonomous exploration, boundary correction, and collaborative recombination create a flexible and robust search mechanism capable of navigating complex and multimodal optimization landscapes effectively.

iv Firmware Update Logic:

In the Drone Squadron Optimization (DSO) framework, the firmware governing each drone is updated dynamically based on both performance evaluation and compliance with operational constraints. The primary criteria for firmware updates are the evaluation of the cost function, which quantifies the effectiveness of a drone's current search strategy, and the detection of any violations of the predefined search boundaries. The Command Center monitors the performance of all drone firmware and identifies the least effective versions. These underperforming firmware modules are then replaced with modified versions derived from the highest performing firmware, subject to a set of conditions to ensure robustness and consistency. The update mechanism is constrained by both node and team counts to maintain proper allocation and avoid overpopulation in any segment of the search process. Mathematically, an update occurs only if the performance metric of a candidate firmware $S(P_k)$ satisfies:

$$S(P_k) > S_{least} \text{ and } S(P_k) > S_{high} \qquad \ldots (8)$$

This ensures that only firmware with demonstrably superior performance contributes to the subsequent search iterations. Furthermore, parameter assignments within the updated firmware must be unique to prevent redundancy and maintain diversity across the drone population. All updates are required to be syntactically valid, guaranteeing that drones can execute the revised firmware without computational errors or operational failures. By systematically replacing low-performing firmware with improved versions, the DSO algorithm achieves a balance between exploitation of successful strategies and exploration of new search trajectories. The structured update mechanism enhances robustness, prevents premature convergence, and ensures steady progression toward global optimal solutions. Overall, the firmware update logic serves as a critical adaptive mechanism that underpins the efficiency, reliability, and convergence performance of the DSO framework in complex optimization scenarios.

v Iteration Control and Stagnation Handling:

Within the Drone Squadron Optimization (DSO) framework, stagnation is identified when the best value of the objective function remains unchanged over a specified number of iterations. This indicates that the swarm may be trapped in a local optimum, requiring adaptive strategies to restore search diversity. To address this, the algorithm implements several mechanisms. First, conflictive coordinates are generated to redirect drones away from regions of local optima, promoting exploration of previously unvisited areas. Second, the algorithm retains a record of search trajectories and plans, enabling the redeployment of successful strategies in subsequent iterations. Third, drones enter a diversification mode, in which random perturbations are applied to their movement patterns to increase variability across the swarm. These adaptive mechanisms collectively enhance the robustness of the DSO algorithm. By introducing controlled randomness and leveraging historical search information, the swarm is able to escape local traps while maintaining convergence toward the global optimum. Consequently, iteration control and stagnation handling ensure that the optimization process remains both dynamic and efficient, particularly in complex or multimodal search landscapes.

### 3.2 MPPT using DSO

The proposed DSO-based MPPT algorithm employs multiple drones, each representing a candidate operating point for the PV converter. Initially, four drones are assigned distinct duty cycles to explore the solution space effectively. Each drone evaluates the instantaneous power using following equation:

$$P = V_{pv} \times I_{pv} \quad \dots (9)$$

After that updates its personal best whenever a higher power output is observed, ensuring retention of optimal results at the individual level. Search iteration is managed via a counter and index, with each duty cycle maintained for 300 iterations to allow stable power evaluation. After completing a cycle, the duty cycle yielding the highest power is designated as the global best, which guides subsequent updates across all drones. Velocity updates are performed using recombination strategies, blending personal and global bests to generate new search directions. Corresponding duty cycles are then updated based on these velocities and constrained within the range of 0.1 to 1.0, ensuring stability and safe operation. The duty cycle achieving the maximum power is applied to the PWM generator, which drives the boost converter toward the MPP. This approach balances exploration and exploitation, enabling efficient and reliable tracking of the global maximum power point even under partial shading conditions. The methodology ensures rapid convergence while maintaining robustness against dynamic environmental variations.

### 3.3 Proposed Hybrid PO-DSO MPPT

A hybrid MPPT control design that combines the DSO and P&O methods to ascertain the ideal duty cycle for a boost regulator is shown in Fig. 6. In this controller configuration, both MPPT blocks receive the Vpv and Ipv at the same time. Based on their own control strategies, each algorithm separately determines a duty cycle. The PO algorithm performs local tracking by fine-tuning around the current operating point, effectively exploiting the nearby power slope to converge on the local maximum. In contrast, the DSO algorithm conducts a global search, exploring a broader region of the operating space to identify the global maximum, which is particularly advantageous under complex, multi-peak conditions such as partial shading. The outputs from the PO and DSO modules are then combined through either an averaging or weighted mechanism to generate a refined duty cycle, which is supplied to the PWM generator. This combined signal ensures that the boost converter operates at an optimized point, leveraging the precise local adjustments of PO while incorporating the global exploration capability of DSO. By integrating these complementary strategies, the hybrid approach achieves enhanced tracking accuracy, faster convergence, and improved robustness against dynamic environmental conditions, including rapid irradiance fluctuations or partial shading events. Consequently, the proposed system not only mitigates the limitations of conventional hill-climbing MPPT methods but also maximizes energy extraction from the PV array across varying operational scenarios, demonstrating superior performance compared to individual PO or DSO implementations.

## 4 Results

The effectiveness of the proposed hybrid PO-DSO MPPT technique is evaluated through simulation tools to detect potential problems early and enhance real-time performance. The performance of the proposed hybrid PO-DSO MPPT controller is tested across

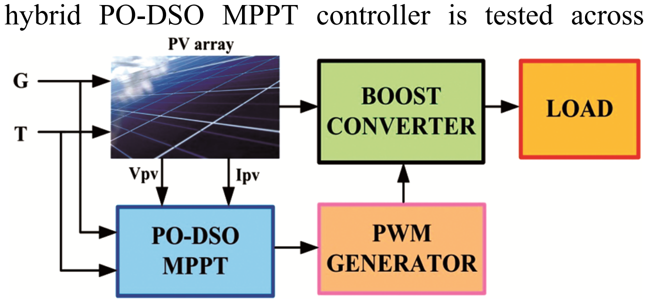


Fig. 6 — Block diagram of the proposed hybrid scheme

various operating scenarios, including Constant irradiance, varying temperature and partial shading conditions. After that a robustness assessments involving random variations in both irradiance and temperature combined with a probabilistic load distribution. The performance of the proposed method is further compared PSO, CS, and FPA, across these scenarios. The comparative performance of proposed hybrid PO-DSO method is evaluated and compared with conventional algorithms, such as PSO, CS and FPA methods across above different scenarios. The value of tracking efficiency ($\eta_{tracking}$) of the different MPPT approach is determined using Eq. (10). Tracking begins at the time $t_1$ and ends at time $t_2$, with the value of average output with the average output power during this interval denoted as $P_{avg}$. Additionally, load-related parameters are monitored and analyzed for each scenario to provide a comprehensive assessment of system performance.

$$\eta_{tracking} = \frac{\int_{t1}^{t2} P_{avg} dt}{\int_{t1}^{t2} P_M dt} \quad \ldots (10)$$

i Case-1 Constant Irradiance & Temperature (1000W/m$^2$ and 25°C)

The solar PV parameter as well as load parameter for the system using proposed hybrid PO-DSO MPPT technique are displayed in Fig. 7 and Fig. 8 under constant irradiance (1000 W/m$^2$) and temperature (25°C). The obtained PV power comparison of hybrid PO-DSO, PSO, CS and FPA MPPT techniques under this condition is shown in Fig. 9. This clearly confirms that the proposed hybrid technique has the least fluctuation around maximum power point (MPP) compare to all other techniques. Also, the greatest PV power that can be achieved using Hybrid PO-DSO is 249.5 W with a smooth and stable convergence. Although PSO also achieves a near a similar but some lesser power level, it exhibits significant oscillations before settling. In contrast, CS and FPA converge earlier but settle at lower power values, around 230.56 W and 243.63 W, respectively. The tracking speed of different MPPT techniques are shown in Fig. 10 under this condition. The proposed hybrid PO-DSO algorithm take very less time to track the MPP as compared to PSO, CS and FPA algorithm. The PV current rises gradually and converges to around 8 A, while the PV voltage begins at about 18 V and stabilizes just above 30 V. The load power is 243.68 W, as seen in Fig. 8. With minor initial oscillations that subside after about 0.6 seconds, the load voltage quickly rises from zero and stabilizes at 90 V. Similar to this, the load current begins at zero,

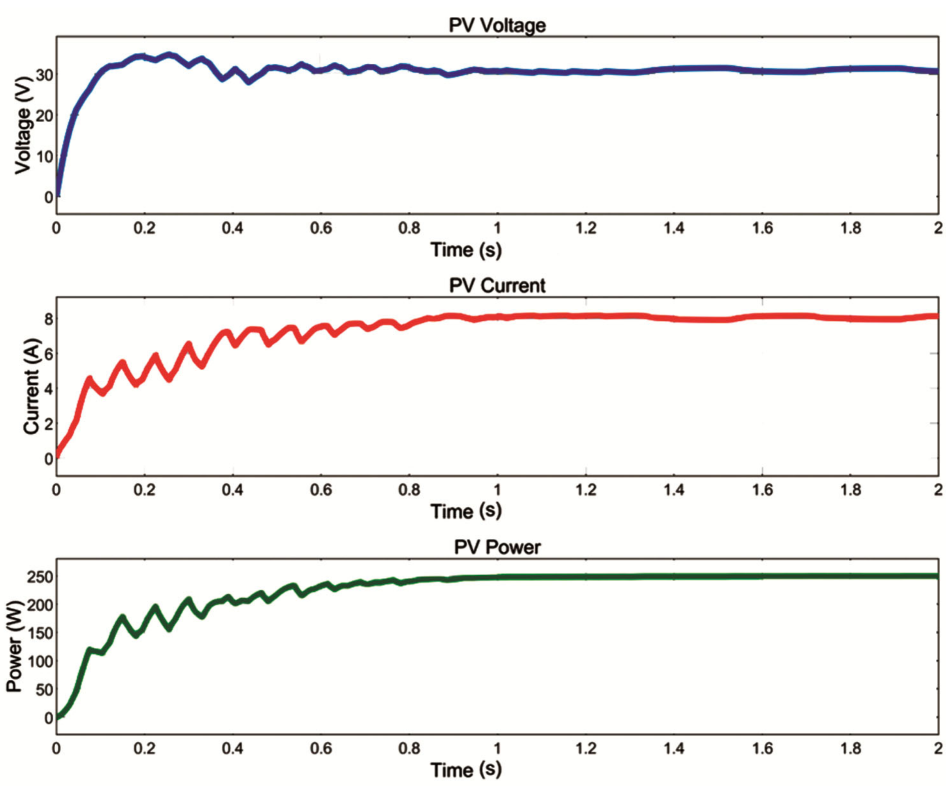


Fig. 7 — PV parameters using hybrid PO-DSO at uniform irradiance

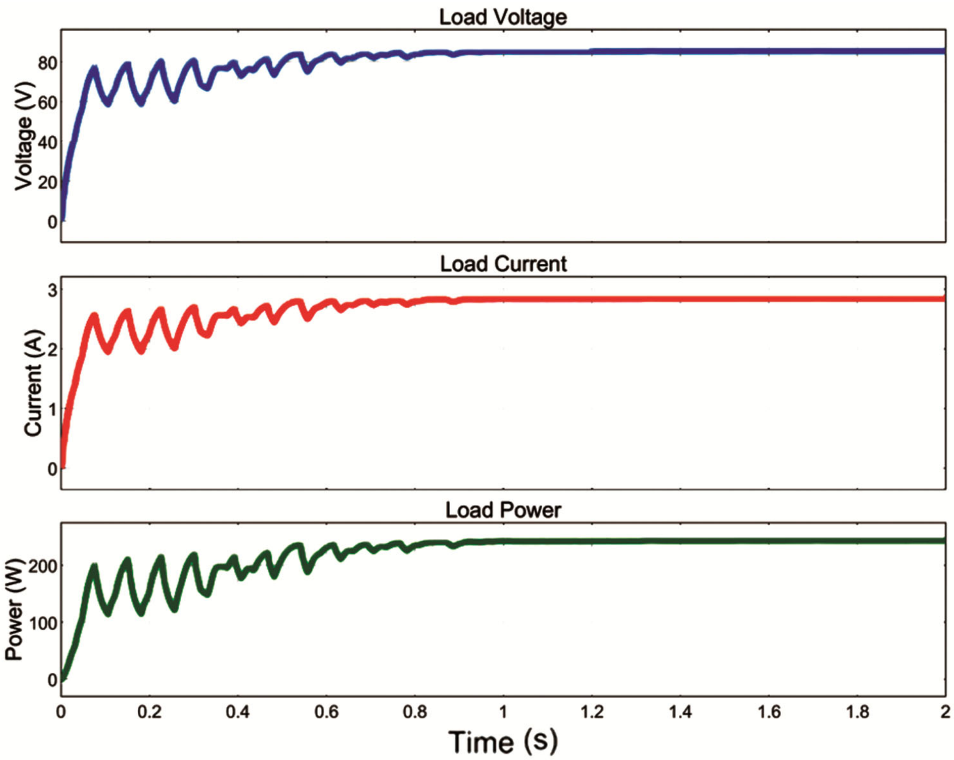


Fig. 8 — Load parameters using hybrid PO-DSO at uniform irradiance

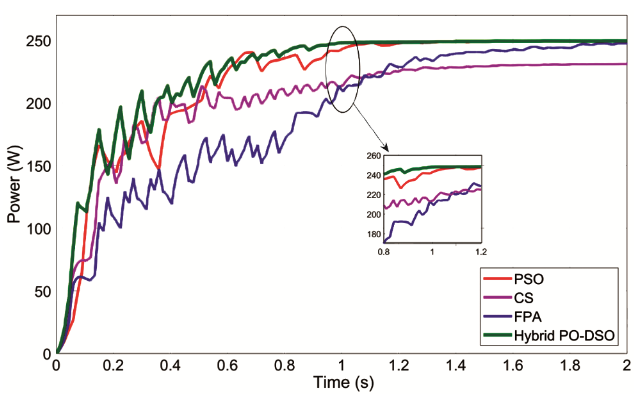


Fig. 9 — PV power comparison of PSO, CS, FPA and proposed hybrid PO-DSO at uniform irradiance

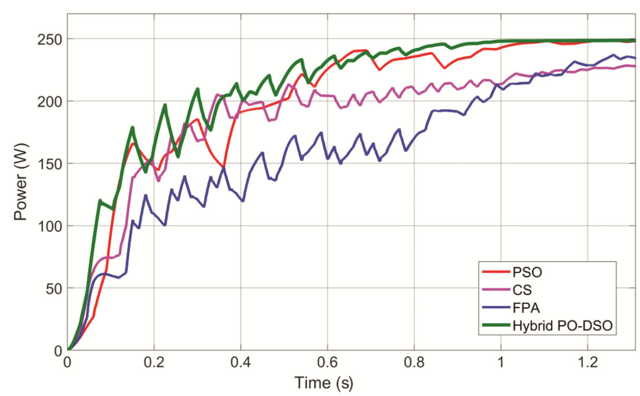


Fig. 10 — Tracking speed comparision of PSO, CS, FPA and proposed hybrid PO-DSO at uniform irradiance

ripples briefly as a result of switching transients, and then settles at 2.5 A. The efficiency curve for different technique under this condition was shown in Fig. 11. Efficiency is calculated as the ratio of actual output power to theoretical power. Under this condition of constant insolation and temperature, hybrid PO-DSO method achieves the highest efficiency (99.87 %), as compare to PSO (99.83 %), CS (92.29 %) and FPA (97.52 %). The curve clearly confirms that the proposed hybrid technique has highest efficiency and was the most efficient under this condition as compare to other three techniques.

ii Case-2 Fixed irradiance & Varying temperature (1000 w/m$^2$ and temperature is varying as 20°C, 25°C & 30°C)

Under this condition of fixed insolation (1000 W/m$^2$) and random temperature, the solar PV parameter as well as load parameter using hybrid PO-DSO MPPT technique is shown in Figs. 12-13, respectively. In this case the value of solar insolation is fixed as 1000 W/m$^2$ for all three panel but temperature is different as 20° C, 25 °C & 30 °C. The output PV power comparison of hybrid PO-DSO, PSO, CS and FPA MPPT techniques under this condition is shown in Fig. 14. This zoom view clearly confirms that the proposed hybrid technique exhibits least oscillation compare to all other techniques around maximum power point (MPP). Here, the Hybrid PO–DSO and PSO again achieve the highest output power (249.3 W and 249.2 W), with Hybrid PO–DSO showing a more stable response. CS and FPA trail behind with lower power values (230.6 W and 243.7 W), and both exhibit mild oscillations during convergence. Figure 15 shows the tracking speed of different MPPT techniques under this condition. Here again, the proposed hybrid PO-DSO algorithm take very less time to track the MPP as compared to PSO, CS and FPA algorithm. The PV current rises gradually and converges to around 8.1 A, while the PV voltage starts at about 17 V and reaches steady state just near 30 V. As per Fig. 12, the load power is near 243.5 W. When the temperature changes, there is only a slight variation in power compared to the last case. With very small initial oscillations that decrease after about 0.65 seconds, the load voltage quickly rises from zero and stabilizes at 85 V. Similar to load voltage, the load current starts at zero, with some ripples as a result of switching transients, and after that settles at 2.6 A. Figure 16 shows the efficiency curve for different technique under this condition. Efficiency is measured by calculating as the ratio of actual output power to theoretical power. Here, in this condition of constant insolation and different temperature, the proposed hybrid PO-DSO method again achieves the highest efficiency (99.80 %), as compare to PSO (99.7 %), CS (92.31 %) and FPA (97.55 %). This consistent

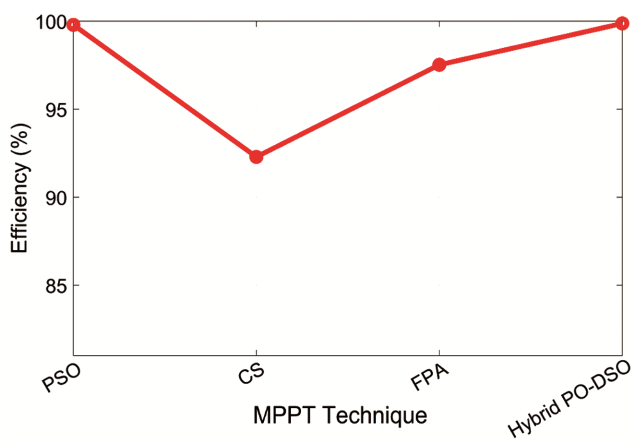


Fig. 11 — Tracking efficiency comparison of PSO, CS, FPA and proposed hybrid PO-DSO at uniform irradiance

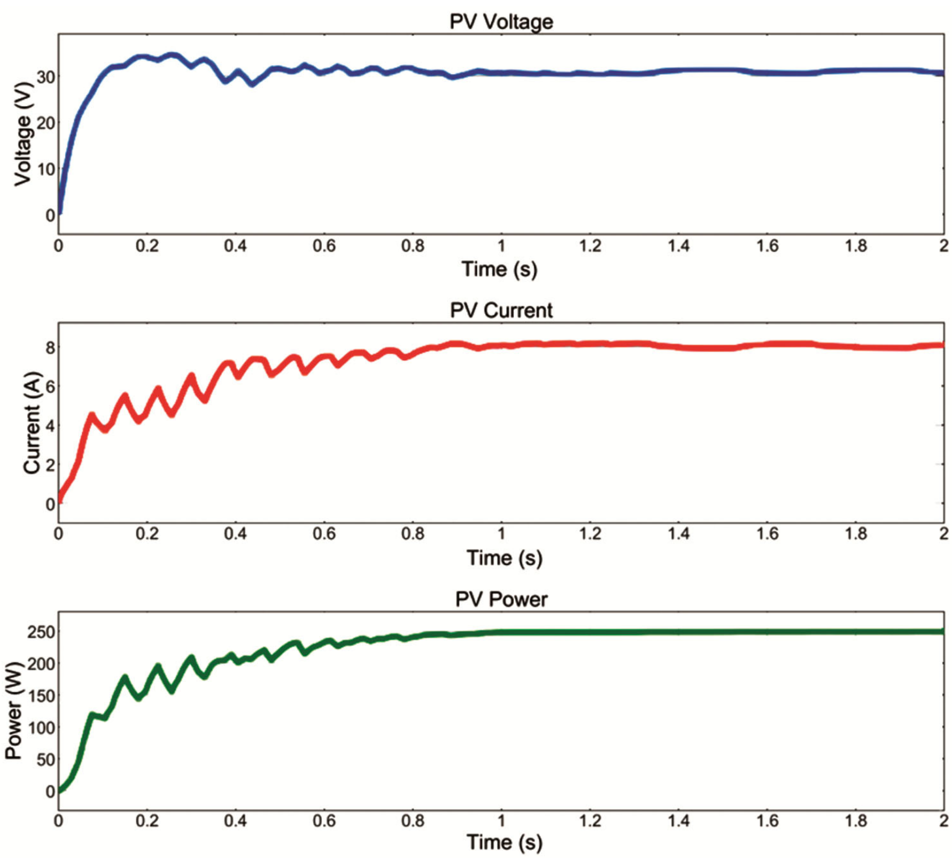


Fig. 12 — PV parameter using hybrid PO-DSO at varying temperature

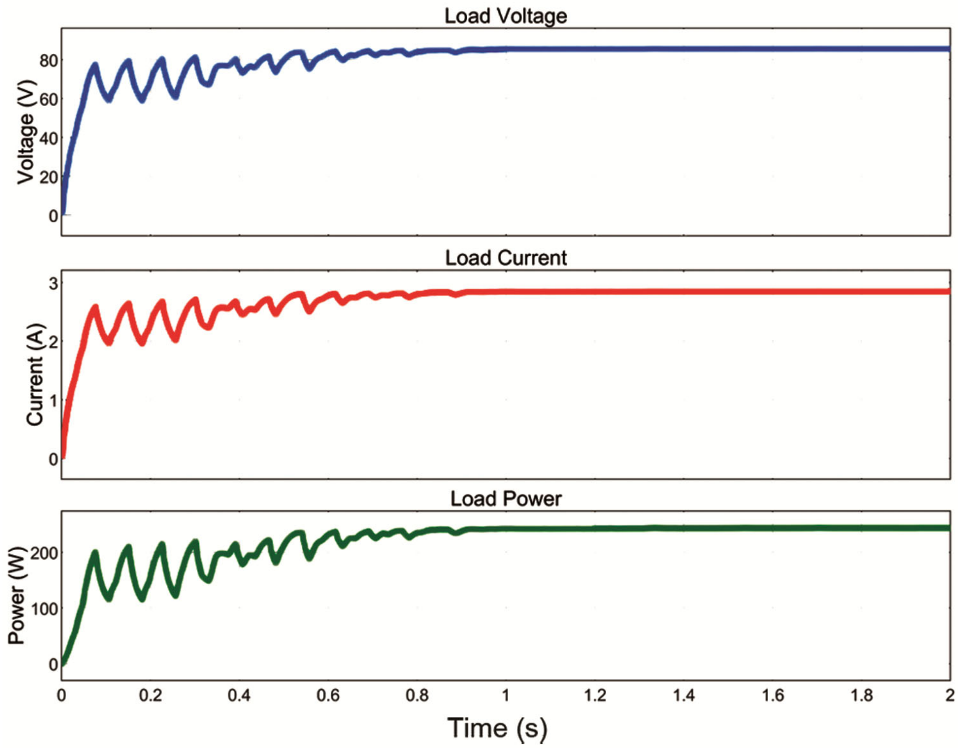


Fig. 13 — Load parameters using hybrid PO-DSO at varying temperature

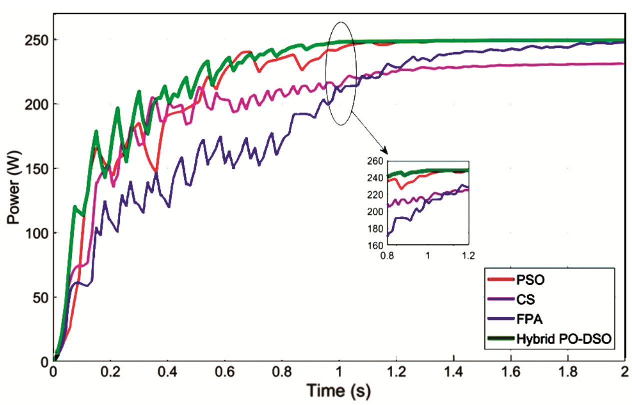


Fig. 14 — PV power comparison of PSO, CS, FPA and proposed hybrid PO-DSO at varying temperature

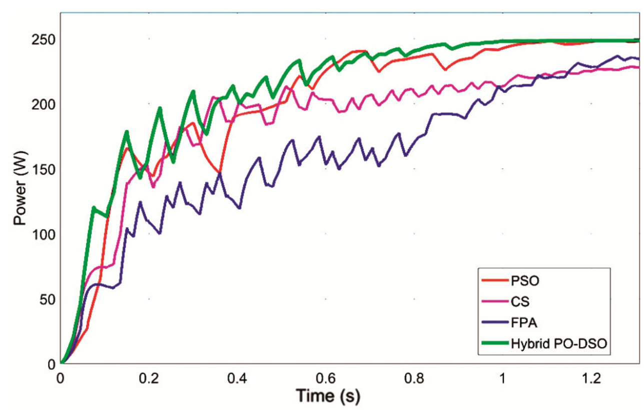


Fig. 15 — Tracking speed comparison of PSO, CS, FPA and proposed hybrid PO-DSO at varying temperature

high efficiency across this condition shows the hybrid PO-DSO MPPT control capability to optimize energy extraction effectively compared to other methods.

iii Case-III Partial Shading Condition-I (Where Panel-1 receives 1000 W/m², Panel-2 receives 250 W/m² and Panel-3 is exposed to 750 W/m² & temperature is fixed in all panels at 25 °C)

Partial shading condition (PSC) is applied by introducing different irradiance levels across a 3-panel PV system. Panel-1 receives 1000 W/m², Panel-2 receives 250 W/m², and Panel-3 is exposed to 750 W/m². The I-V as well as P-V characteristics of partial shaded solar PV model for this case is shown in Fig. 17, Where there is two LMPP and one GMPP presents. The PV as well as load parameters for this condition of partial shading is shown in Figs. 18-19, respectively. As shown in Fig. 17, the PV parameters under this condition yield a maximum power output of 128.25 W using the Hybrid PO-DSO technique. Correspondingly, the load power, illustrated in Fig. 18, reaches 124.31 W, demonstrating the system's effective performance despite non-uniform irradiance. The PV power output using PSO, CS and FPA is 127.8 W, 116.41W and 124.34 W, as which is lesser than the proposed method. Figure 20 shows the output PV power comparison of hybrid PO-DSO, PSO, CS and FPA MPPT techniques under this partial shading condition The zoom view represents a more constrained case where the Hybrid PO–DSO and PSO both reach nearly same power output, but the Hybrid PO–DSO achieves some high value with less oscillatory behavior. FPA follows with 124.34 W, and CS lags at 116.41 W, reflecting reduced efficiency. The tracking speed of different MPPT techniques under partial shading condition is shown in Fig. 21.

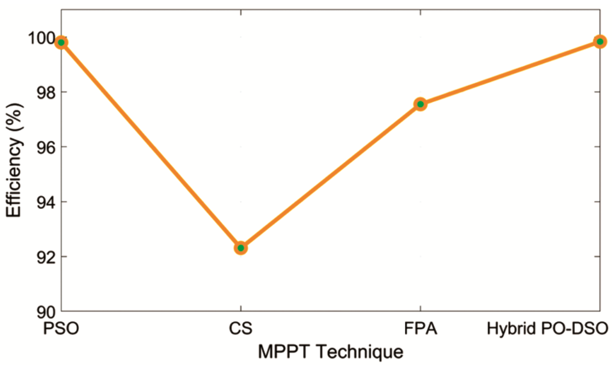


Fig. 16 — Tracking efficiency comparison of PSO, CS, FPA and proposed hybrid PO-DSO at varying temperature

The Fig. 21 shows that the proposed hybrid PO-DSO MPPT technique takes least time to track the maximum power point as compared to PSO, CS and FPA algorithm. Using proposed method, the PV current increases continuously and gradually and converges to around 6.1A, whereas the PV voltage starts at about 19 V and reaches stable value just near 21 V in about 0.7seconds. The Fig. 19 shows that the

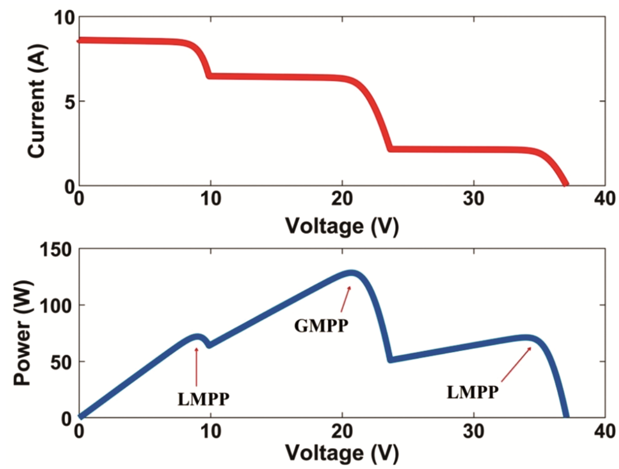


Fig. 17 — I-V and P-V characteristics of partial shaded solar PV model

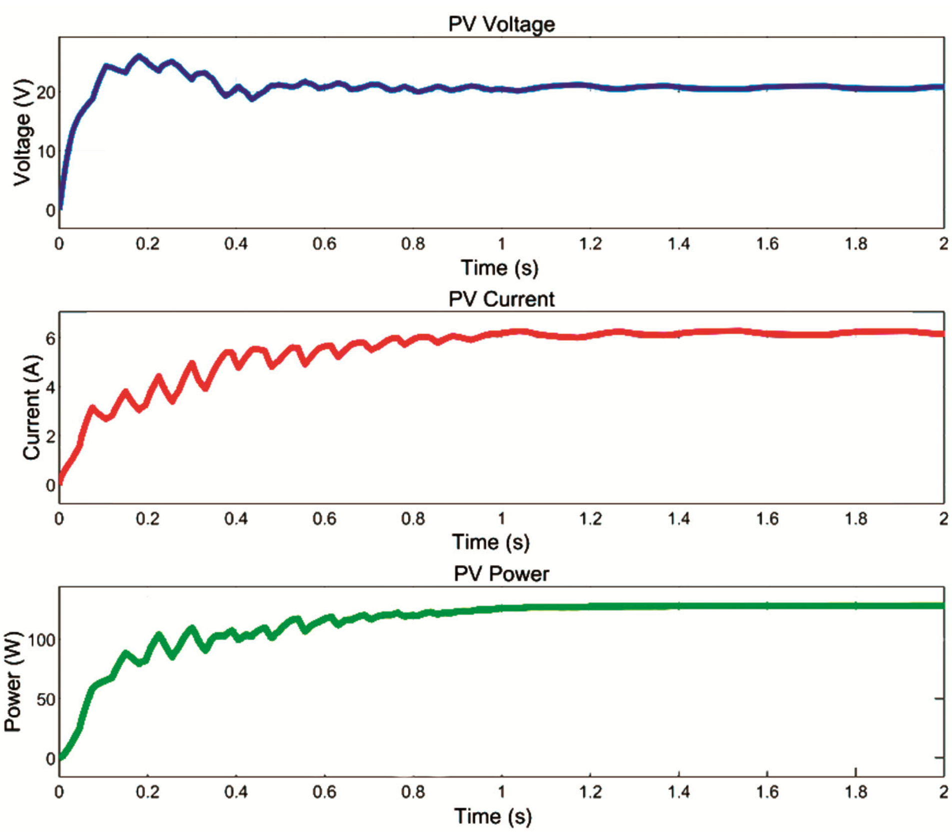


Fig.18 — PV parameters using hybrid PO-DSO at PSC-I

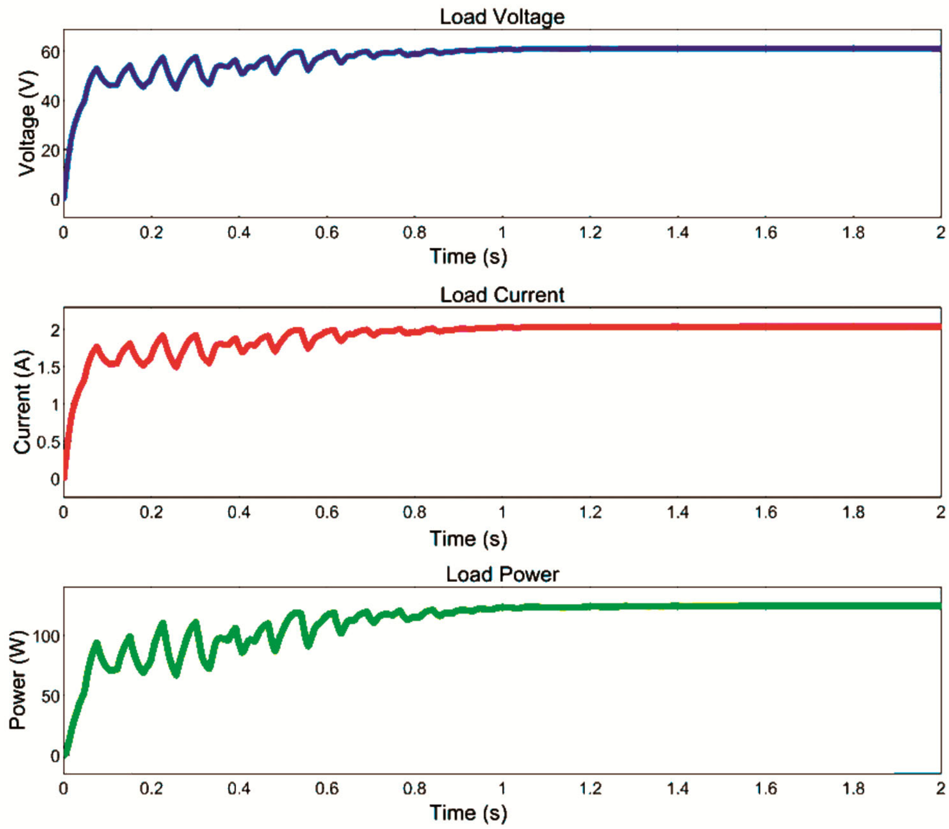


Fig. 19 — Load parameters for hybrid PO-DSO at PSC-I

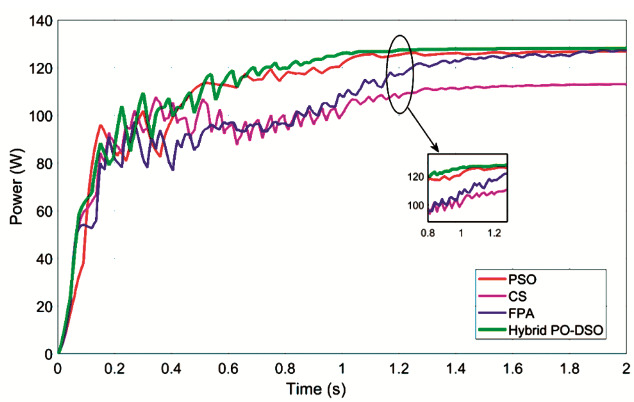


Fig. 20 — PV power comparison of PSO, CS, FPA and proposed hybrid PO-DSO at PSC-I

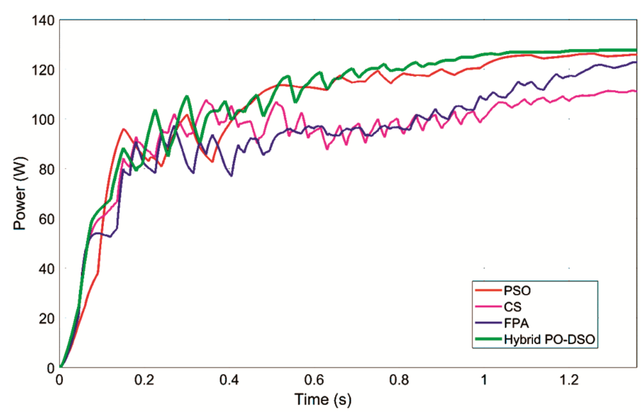


Fig. 21 — Tracking speed comparison of PSO, CS, FPA and proposed hybrid PO-DSO at PSC-I

load power is near 124.31 W in this partial shading condition. The load voltage in this PSC having very small initial fluctuations that decrease after about 0.7 seconds, the load voltage quickly rises from zero and stabilizes at near 61 V. Like load voltage, the load current starts at zero, with some initial ripples as a result of PSC, and after that settles at 2.03 A. The efficiency curve under this partial shading condition (PSC) using different MPPT technique is shown in Fig. 22. Efficiency is find out by calculating the ratio of actual output power to theoretical power. Here, in this condition of PSC, the proposed hybrid PO-DSO method once again achieves the highest efficiency (99.88 %), as compare to PSO (99.53 %), CS (90.66 %) and FPA (96.84 %). This consistent high efficiency across this partial shading condition shows the hybrid PO-DSO MPPT control capability to optimize energy extraction effectively compared to other methods. The superior efficiency result under partial shading conditions of the proposed hybrid

PO-DSO MPPT methods proving its strong ability to extract energy more effectively than other methods.

iv Case-IV: Partial Shading Condition-II (Where Panel-1 receives 1000 W/m², Panel-2 receives 250 W/m², and Panel-3 is exposed to 750 W/m² & temperature is also different as 20 °C, 25 °C & 30 °C)

In this scenario, a three-panel photovoltaic (PV) system was subjected to a deliberate partial shading condition by imposing non-uniform irradiance and varying temperature levels across the modules. Panel-1 received an irradiance of 1000 W/m² at a temperature of 20 °C, Panel-2 operated under 250 W/m² at 25 °C, and Panel-3 was exposed to 750 W/m² at 30 °C. The I-V as well as P-V characteristics of partial shaded solar PV model for this case is shown in Fig. 23, Where there is two LMPP as well as one GMPP presents. The corresponding PV and load characteristics under this shading condition are presented in Figs 24-25. As

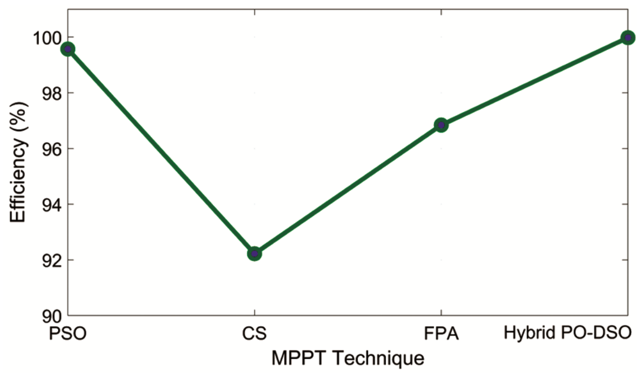


Fig. 22 — Tracking efficiency comparison of PSO, CS, FPA and proposed hybrid PO-DSO at PSC-I

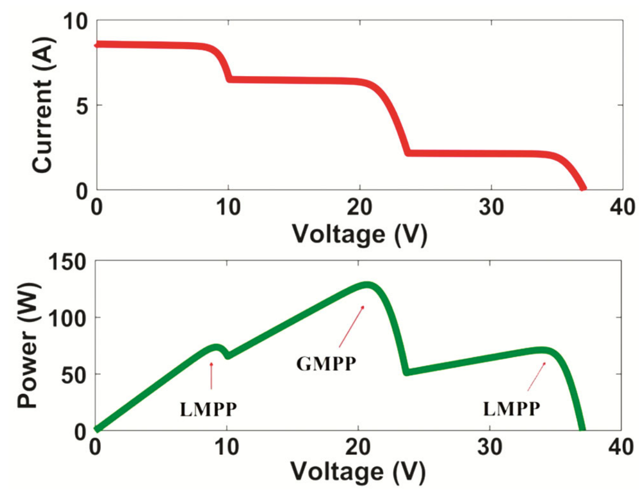


Fig. 23 — I-V and P-V characteristics of partial shaded solar PV model for PSC-II

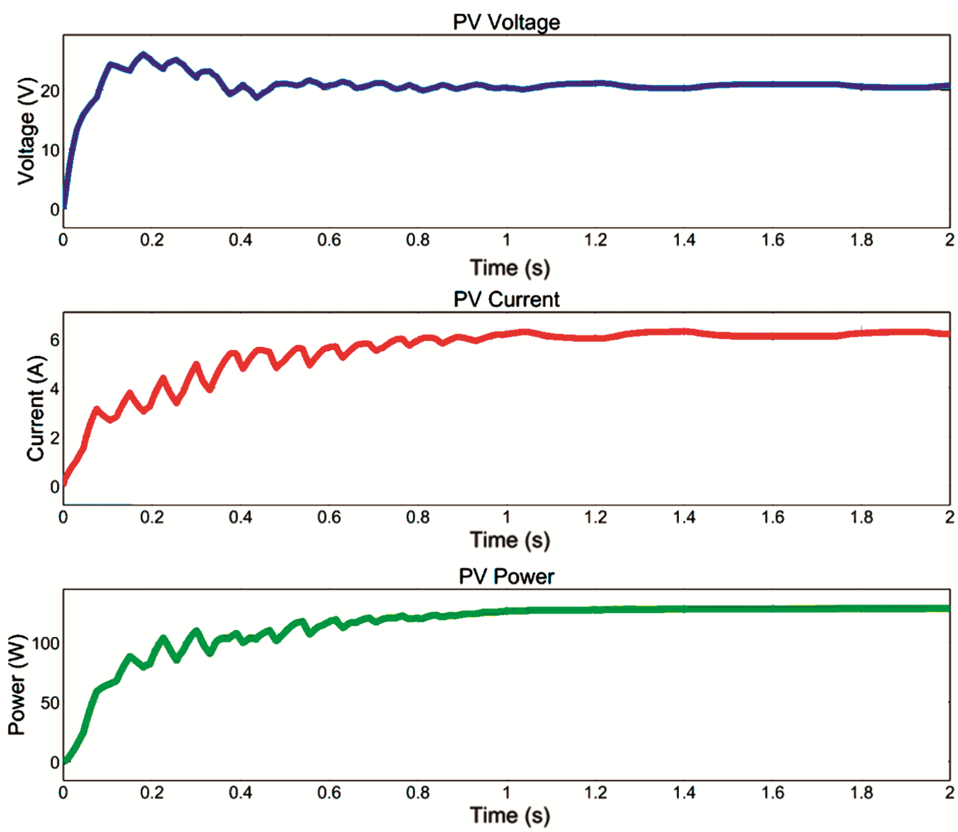


Fig. 24 — PV parameters using hybrid PO-DSO at PSC-II

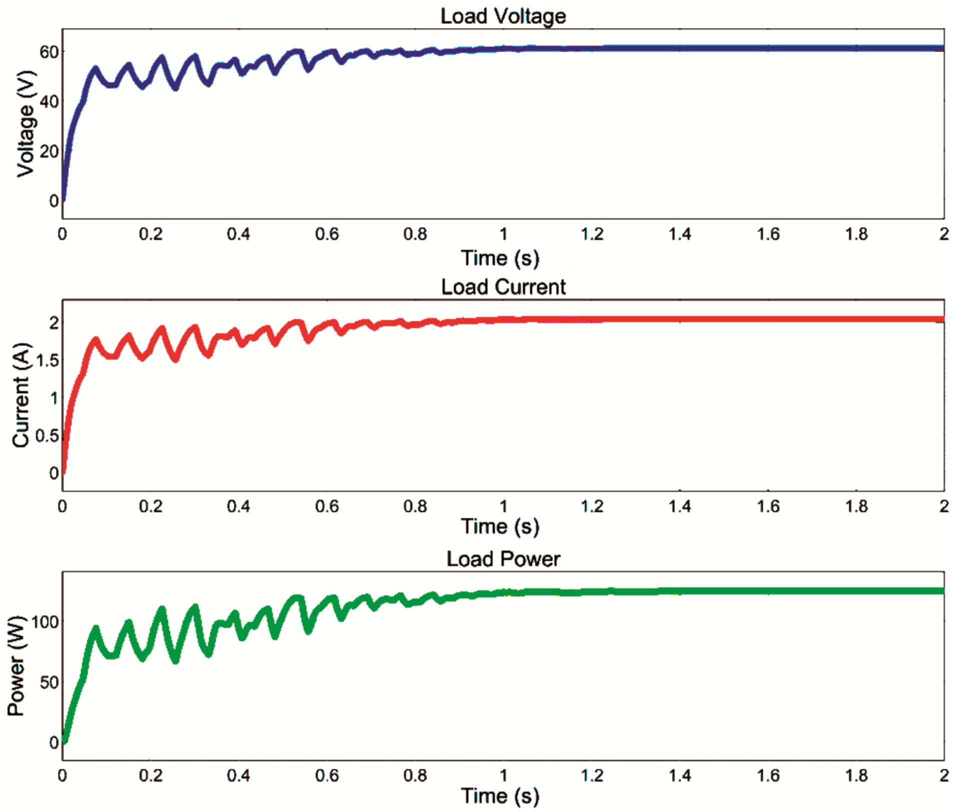


Fig. 25 — Load parameters using hybrid PO-DSO at PSC-II

depicted in Fig. 24, the proposed Hybrid PO-DSO technique yielded a maximum PV power output of 128.3 W. The corresponding load power, shown in Fig. 25, achieved a value of 124.2 W, highlighting the ability of the proposed method to maintain strong performance despite irradiance and temperature mismatches. For comparison, conventional optimization techniques like PSO, CS, and FPA produced lower maximum power values of 127.3 W, 112.8 W, and 123.54 W, respectively. A comparative illustration in Fig. 26 confirms that while PSO approaches the proposed method in terms of power yield, the Hybrid PO-DSO algorithm exhibits superior stability with less oscillatory behavior. In contrast, FPA and CS demonstrated reduced efficiency under the same conditions. The tracking speed performance of the four methods under partial shading is presented in Fig. 27. This shows that the proposed Hybrid PO-DSO MPPT technique shows the fastest convergence towards the maximum power point (MPP) as compared to other conventional techniques such as PSO, CS, and FPA. During the tracking process, the PV current illustrated a gradual and stable rise, ultimately settling at a value equals to approximately 6.2 A. At the same time, the PV voltage increased

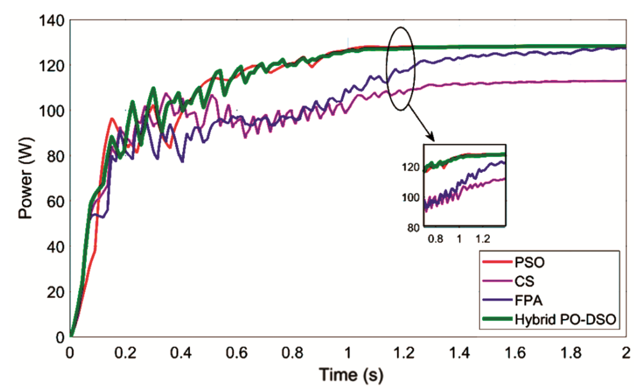


Fig. 26 — Power comparison of PSO, CS, FPA and proposed hybrid PO-DSO at PSC-II

smoothly from an initial value of 17 V to a nearly of 21 V within a time frame of 0.8 seconds, highlighting the superior dynamic response and stability of the proposed hybrid method. Similarly, the load parameters reflected stable behavior as the load power settled at 124.2 W, the load voltage stabilized near 60 V after minor initial transients, and the load current converged around 2.0 A. The efficiency analysis, illustrated in Fig. 28, was conducted by evaluating the ratio of actual output power to theoretical maximum power. The result shows that the

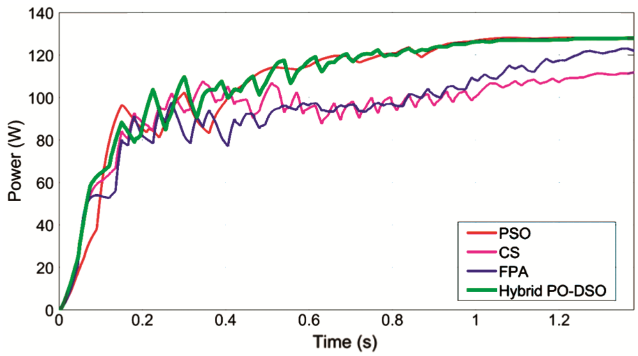


Fig. 27 — Tracking speed comparison of PSO, CS, FPA and proposed hybrid PO-DSO at PSC-II

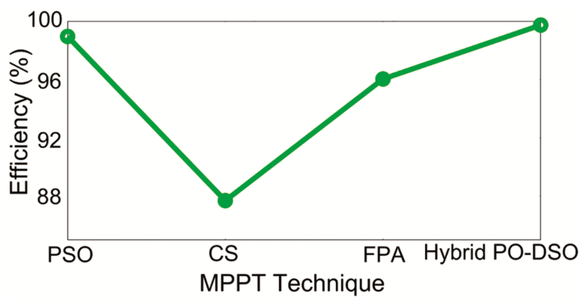


Fig. 28 — Efficiency comparison of PSO, CS, FPA and proposed hybrid PO-DSO at PSC-II

proposed Hybrid PO–DSO technique consistently delivered the highest efficiency of 99.74 % under partial shading conditions. The proposed hybrid PO-DSO MPPT approach outperforms PSO, FPA, and CS, which achieved efficiencies of 98.96 %, 87.69 %, and 96.04 %, respectively, by ensuring faster convergence and reduced oscillations. Consequently, the algorithm ensures stable and highly efficient energy extraction, even under adverse challenging conditions such as partial shading and also non-uniform irradiance within the PV array.

### 4.1 Robustness Test Under Partial Shading Condition with Probabilistic Distribution of Load

The robustness of the proposed hybrid PO-DSO algorithm was evaluated through tests conducted under dynamically varying operating conditions, including random fluctuations in solar irradiance, temperature, and probabilistic load variations. The integration of a probabilistic load distribution signal in the robustness assessment is particularly significant in context of MPPT analysis, as it enables a comprehensive evaluation of the PV system's capability and its controller's adaptability in handling uncertain and non-deterministic real-world environments. Load variations were applied in three successive stages to emulate realistic operating

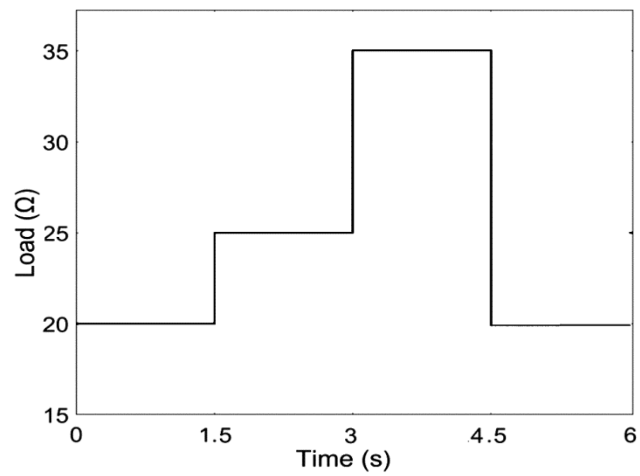


Fig. 29 — Probabilistic distribution signal of load

disturbances: an initial minor shift at 5 Ω, followed by a moderate change at 10 Ω, and finally, a significant variation at 15 Ω. The load resistance was further modeled using a probabilistic distribution with values of 20, 25, 35, and 20 Ω, updated at intervals of 1.5 seconds. Figure 29 depicts the probabilistic load distribution signal, while Fig. 30 (a–d) presents the PV power curve, tracking response, PV current, and PV voltage obtained from different MPPT algorithms during reliability assessment. The corresponding Power losses under each condition were calculated using Eq. (11), where $t$ represents the convergence time required to reach the Maximum Power Point (MPP). For a more detailed assessment of tracking precision, three statistical indices were employed: root mean square error (RMSE), mean relative error (MRE), and mean absolute percentage error (MAPE), calculated according to Eqs. (12) -(14), where $n$ represents the total number of data samples[27]. The outcomes of this evaluation confirm that the proposed hybrid PO-DSO approach exhibits greater robustness and adaptability than conventional MPPT techniques when subjected to both deterministic and probabilistic operating conditions.

$$\text{Power loss} = \frac{\sum P_M(t) - \sum P(t)}{\sum P_M(t)} \times 100\% \quad \ldots (11)$$

$$\text{RMSE} = \sqrt{\frac{\sum(\text{actual} - \text{estimated})^2}{n}} \quad \ldots (12)$$

$$\text{MRE} = \frac{|\,\text{Actual value} - \text{Estimated value}\,|}{\text{Actual value}} \quad \ldots (13)$$

$$\text{MAPE} = \frac{1}{n}\sum\frac{|\,\text{Actual value} - \text{Forcasting}|}{|\,\text{Actual}\,|} \times 100\% \quad \ldots (14)$$

Table 2 highlights that the proposed hybrid PO-DSO controller achieves superior performance

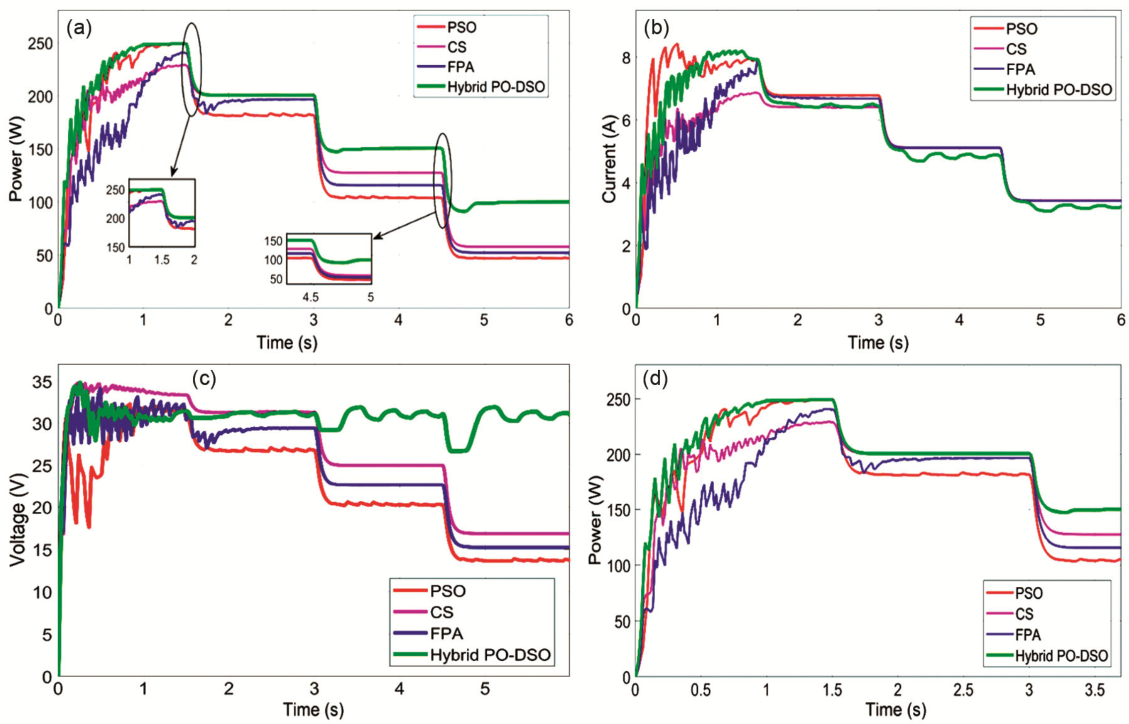


Fig. 30 — Under partial shading condition with probabilistic distribution of load (a) PV power (b) PV current (c) PV voltage and; (d) Tracking speed

Table 2 — Comparison under robustness test in different states

| MPPT technique | State 1<br>1-1.5sec | State 2<br>1.5-3sec | State 3<br>3-4.5sec | state 4<br>4.5-6sec |
|---|---|---|---|---|
| *Average actual power (W)* | | | | |
| PSO | 249.4 | 183.6 | 104.8 | 47.8 |
| CS | 230.56 | 200.6 | 127.5 | 58.27 |
| FPA | 240.9 | 196.5 | 116.1 | 52.76 |
| Hybrid PO-DSO | 249.5 | 200.7 | 150.17 | 99.63 |
| *Tracking time (s)* | | | | |
| PSO | 1.410 | 0.5482 | 0.549 | 0.673 |
| CS | 1.471 | 0.335 | 0.408 | 0.434 |
| FPA | 1.458 | 0.760 | 0.273 | 0.479 |
| Hybrid PO-DSO | 1.143 | 0.249 | 0.119 | 0.362 |
| *Tracking efficiency (%)* | | | | |
| PSO | 99.81 | 91.44337 | 69.491 | 47.75 |
| CS | 92.27 | 99.9103 | 84.543 | 58.20 |
| FPA | 96.41 | 97.86831 | 76.984 | 52.70 |
| Hybrid PO-DSO | 99.8599 | 99.1034 | 99.576 | 99.51 |
| *PV voltage ripple (V)* | | | | |
| PSO | 2.6 | 0.86 | 1.12 | 3.31 |
| CS | 1.44 | 2.06 | 2.36 | 3.01 |
| FPA | 1.78 | 2.33 | 1.33 | 2.14 |
| Hybrid PO-DSO | 0.41 | 0.17 | 0.4 | 0.8 |
| *PV current ripple (A)* | | | | |
| PSO | 0.485 | 0.169 | 0.455 | 0.058 |
| CS | 0.088 | 0.108 | 0.108 | 0.039 |

(*Contd.*)

Table 2 — Comparison under robustness test in different states (*Contd.*)

| MPPT technique | State 1 | State 2 | State 3 | state 4 |
|---|---|---|---|---|
| FPA | 0.417 | 0.054 | 0.055 | 0.025 |
| Hybrid PO-DSO | 0.02 | 0.086 | 0.069 | 0.017 |
| *Root mean square error (RMSE)* | | | | |
| PSO | 0.225 | 8.59 | 23.005 | 26.155 |
| CS | 9.645 | 0.09 | 11.655 | 20.920 |
| FPA | 4.475 | 2.14 | 17.355 | 23.675 |
| Hybrid PO-DSO | 0.175 | 0.09 | 0.32 | 0.242 |
| *Mean relative error (MRE)* | | | | |
| PSO | 0.0056 | 0.0215 | 0.0488 | 0.0698 |
| CS | 0.0072 | 0.0251 | 0.0421 | 0.0727 |
| FPA | 0.0128 | 0.0237 | 0.0468 | 0.2577 |
| Hybrid PO-DSO | 0.0024 | 0.0205 | 0.0421 | 0.0755 |
| Mean absolute percentage error *(MAPE)* | | | | |
| PSO | 0.005 | 0.086 | 0.3051 | 0.5225 |
| CS | 0.077 | 0.013 | 0.1546 | 0.4179 |
| FPA | 0.036 | 0.021 | 0.2302 | 0.4729 |
| Hybrid PO-DSO | 0.002 | 0.009 | 0.0042 | 0.0048 |
| *Average power output (W)* | | | | |
| PSO | 242.6 | 176.8 | 100.6 | 45.29 |
| CS | 224.6 | 195.7 | 124.0 | 55.79 |
| FPA | 236.6 | 191.6 | 112.5 | 50.47 |
| Hybrid PO-DSO | 243.7 | 196.1 | 146.7 | 96.93 |
| *Power loss (%)* | | | | |
| PSO | 0.18 | 8.556 | 30.5085 | 52.25 |
| CS | 7.72 | 0.0897 | 15.4565 | 41.79 |
| FPA | 3.582 | 2.33 | 23.0157 | 47.29 |
| Hybrid PO-DSO | 0.14 | 0.089 | 0.4243 | 0.4895 |
| *Overall efficiency (%)* | | | | |
| PSO | 97.10 | 88.07 | 66.71 | 45.24 |
| CS | 89.89 | 97.47 | 82.22 | 55.73 |
| FPA | 94.70 | 95.43 | 74.60 | 50.41 |
| Hybrid PO-DSO | 97.54 | 97.67 | 97.28 | 96.82 |

compared to conventional MPPT techniques. The results indicate significantly lower current and voltage ripples, enhanced output power, shorter tracking time, and higher tracking as well as overall efficiency. Moreover, the method demonstrates reduced power losses and consistent accuracy in locating the Maximum Power Point (MPP) throughout all four operating intervals. Table 2 also contains comparisons of tracking efficiency, the power loss, voltage ripple & current ripple, overall efficiency, tracking duration, accuracy in tracking and associated error values (MRE, RMSE and MAPE). Figure 30 (a-d) shows the the value of PV power, pv current, pv voltage and tracking speed variation. Whereas, Fig. 31 (a-c) shows performance assessment like voltage ripple, current ripple, tracking efficiency, overall efficiency, tracking time & Power loss (%) through graph for robustness test under PSC with probabilistic distribution of load

## 5 Experimental Validation of the Proposed Hybrid PO-DSO controller Under PSC

The proposed hybrid PO-DSO MPPT technique effectiveness was tested experimentally using the OPAL-RT (OP4510) real-time simulator, as shown in Fig. 32. This is a high-performance platform equipped with four processing cores and integrated with the RT-LAB environment, which serves as a key component for real-time implementation. This setup allows accurate assessment of the dynamic response and practical applicability of the proposed MPPT method under different operating conditions. The experimental configuration is organized into two major components, which is the host computer and

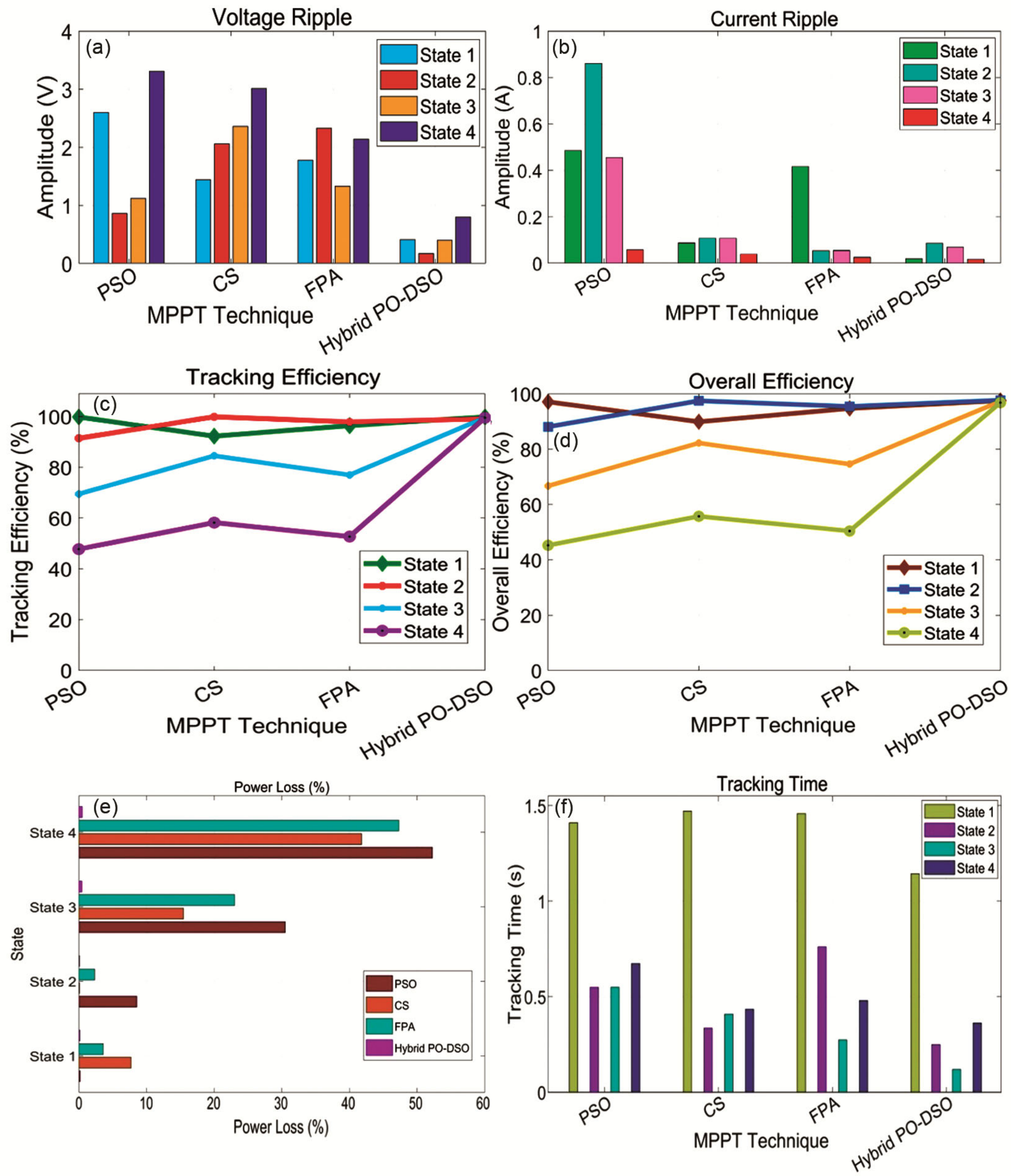


Fig. 31 — Performance assessment through graph for robustness test under PSC (a) Voltage ripple and current ripple **(b)**Tracking and overall efficiency and **(c)** Power loss (%) & tracking time

the real-time (RT) simulator. The RT-LAB environment is responsible for compiling the Simulink model and creating a user interface on the host computer, through which model adjustments and modifications can be performed with ease. Once compiled, the RT simulator ensures real-time execution of the model by interfacing with the host computer via a Telnet connection using dedicated system software. The Simulink model was implemented on the OPAL-RT (OP4510) platform, and experimental validation was performed under partial shading conditions. In this setup, solar panel 1 is operated at 1000 W/m², panel 2 is at 250 W/m², and panel 3 is at 750 W/m². The performance of the hybrid PO-DSO MPPT controller under these conditions is presented in Fig. 33. The proposed controller showed a quick response to PSC, maintained very small oscillations around the maximum power point (MPP), and exhibited minimal ripple. These results demonstrate that the proposed hybrid MPPT controller achieves nearly lossless power tracking, even when subjected to PSC and challenging atmospheric condition.

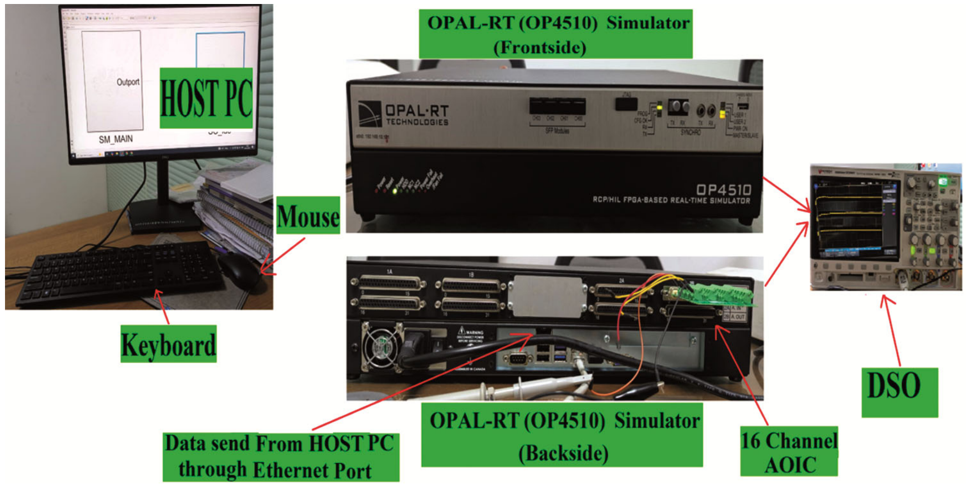

Fig. 32 — The experimental setup for the validation of the proposed hybrid PO-DSO algorithm under PSC

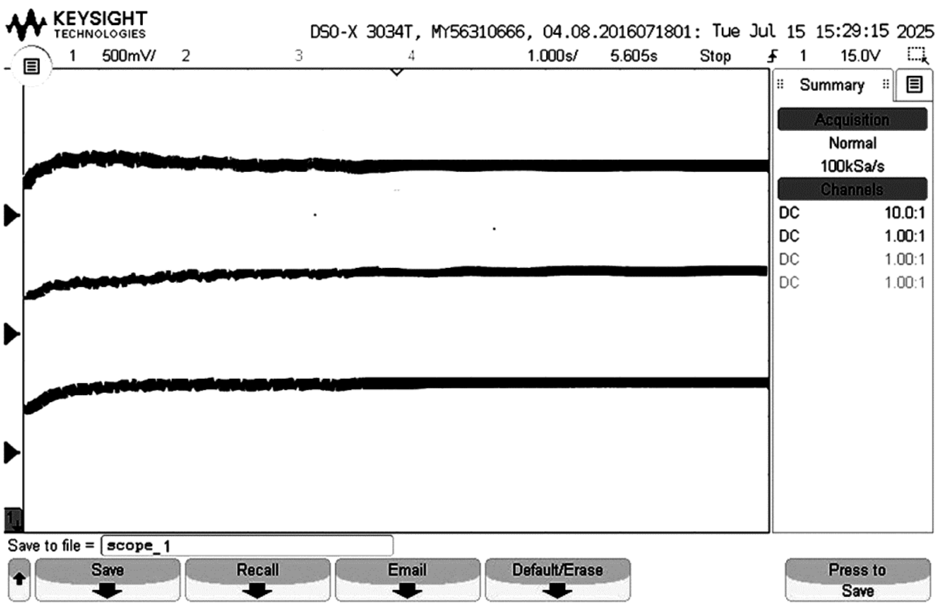

Fig. 33 — Output experimental result of proposed hybrid PO-DSO MPPT under PSC

## 6 Conclusion

The proposed Hybrid PO-DSO MPPT algorithm has been successfully validated through detailed simulation under different operating conditions, including constant insolation, varying temperature, and partial shading conditions. In the constant insolation condition, the hybrid method achieved a PV power output of 249.5 W and delivered 243.68 W to the load, with voltage and current stabilizing quickly with less oscillation. Under varying temperature conditions, it give PV power output of 249.3 W, showing minimal sensitivity to temperature changes. Even in the most challenging scenario of partial shading the proposed method reached a PV power output of 128.25 W and delivered 124.31 W to the load in first PSC case. Also, in second PSC case the proposed hybrid method gives a PV power output of 128.3 W and supplies 124.2 W to the load, showing its capability to track the GMPP effectively despite the existence of multiple local peaks. Comparative analysis with other optimization-based MPPT procedure like PSO, CS, and FPA further highlights the superiority of the proposed method. While PSO achieved comparable peak power values, it suffered from severe steady-state oscillations. CS and FPA, though stable, converged to lower power values. The Hybrid PO–DSO achieved the highest average efficiency across all cases, reaching up to 99.8 %, thus ensuring both accuracy and reliability. Its combined use of local and global search mechanisms enables faster convergence and greater resilience under dynamic environmental conditions. The effectiveness of the controller was additionally validated through real-time experiments using the OP4510 simulator in a laboratory. The experimental results closely corresponded with the simulation result, confirming the proposed method accuracy and practical applicability. After integration of PO with Drone Squadron Optimization (DSO) in the Hybrid PO-DSO MPPT system, a systematic and adaptive framework for enhancing solar PV performance is achieved. This approach not only demonstrates the potential to advance MPPT strategies but also underscores its role in the efficient utilization of solar energy. The Hybrid PO-DSO MPPT system sets a new benchmark for tracking efficiency and energy extraction, contributing to improved reliability and overall performance in photovoltaic energy generation.

| Nomenclature | | Abbreviations | |
|---|---|---|---|
| DSO | Drone squadron optimization | T | Temperature |
| CS | Cuckoo Search Algorithm | G | Solar insolation (W/m$^2$) |
| PV | Photovoltaic | $\eta$ | The tracking efficiency (%) |
| FPA | Flower Pollination Algorithm | k | Boltzmann constant (J/K) |
| MPPT | Maximum power point tracking | | |
| GMPP | Global maximum power point | | |
| LMPP | Local maximum power point | | |
| PSO | Particle swarm optimization | | |
| PSC | Partial shading condition | | |
| PO | Perturb and observe | | |

## References


1 Paraschiv L S & Paraschiv S, *Energy Rep*, 9 (2023) 535.
2 Hassan Q, Viktor P, Al-Musawi T J, Ali B M, Algburi S, Alzoubi H M & Jaszczur M, *Renew Energy Focus*, 48 (2024) 100545.
3 Al-Shetwi A Q, *Sci Total Environ*, 822 (2022) 153645.
4 Olabi A G & Abdelkareem M A, *Renew Sustain Energy Rev*, 158 (2022) 112111.
5 Maka A O & Alabid J M, *Clean Energy*, 6 (3) (2022) 476.
6 Strielkowski W, Civín L, Tarkhanova E, Tvaronavičienė M & Petrenko Y, *Energies*, 14 (24) (2021) 8240.
7 Joisher M, Singh D, Taheri S, Espinoza-Trejo D R, Pouresmaeil E & Taheri H, *IEEE Access*, 8 (2020) 38481.
8 Gao C & Chen H, *Utilities Policy*, 82 (2023) 101543.
9 Bollipo R B, Mikkili S & Bonthagorla P K, *CSEE J Power Energy Syst*, 7 (1) (2020) 9.
10 Bastidas-Rodriguez J D, Franco E, Petrone G, Ramos-Paja C A & Spagnuolo G, *IET Power Electron*, 7 (6) (2014) 1396.
11 Reisi A R, Moradi M H & Jamasb S, *Renew sustain energy rev*, 19 (2013) 433.
12 Bollipo R B, Mikkili S & Bonthagorla P K, *IET Renew Power Generation*, 14 (9) (2020) 1433.
13 Deshkar S N, Dhale S B, Mukherjee J S, Babu T S & Rajasekar N, *Renew Sustain Energy Rev*, 43 (2015) 102.
14 Rajasekar N, Kumar N K & Venugopalan R, *Solar Energy*, 97 (2013) 255.
15 Goyal S K, Sungh B P, Kumar A, Kumar P & Saraswat A, IEEE *International Conference on Computation, Automation and Knowledge Management (ICCAKM)*, 2020 pp. 367.
16 Mohapatra A, Nayak B, Das P & Mohanty K B, *Renew Sustain Energy Rev*, 80 (2017) 854.
17 Rezk H, Fathy A & Abdelaziz A Y, *Renew Sustain Energy Rev*, 74 (2017) 377.
18 Sarvi M & Azadian A, *Energy Syst*, 13 (2) (2022) 281.
19 Sarvi M, Ahmadi S & Abdi S, *Prog Photovoltaics: Res Appl*, 23 (2) (2015) 201.
20 Sangrody R, Taheri S, Cretu A M & Pouresmaeil E, *IEEE Trans Sustain Energy*, 15 (1) (2023) 136.
21 Nouh A, Almalih A H, Faraj M A, Almalih A & Mohamed F, *J Solar Energy Sustain Develop*, 13 (1) (2024) 114.
22 Ibrahim A, Obukhov S & Aboelsaud R, *Appl Solar Energy*, 55 (2019) 367.
23 Tagayi R K, Baek J & Kim J, *J Build Eng*, 66 (2023) 105818.
24 Ahmed J & Salam Z, *Appl Energy*, 150 (2015) 97.
25 de Melo V V & Banzhaf W, *Neural Comput Appl*, 30 (10) (2018) 3117.
26 Mazumdar D, Biswas P K, Sain C, Ahmad F, Ustun T S & Kalam A, *Renew Energy Focus*, 49 (2024) 100577.
27 Pathak P K, Yadav A K & Alvi P A, *J Eng Res*, 11 (2022) 112.